Neurochemistry International 129 (2019) 104500

Contents lists available at ScienceDirect

Neurochemistry International

journal homepage: www.elsevier.com/locate/neuint

# Different epidermal growth factor receptor signaling pathways in neurons and astrocytes activated by extracellular matrix after spinal cord injury

Xin Zhao[a,b,1], Zexiong Li[c,1], Shanshan Liang[c], Shuai Li[c], Jiaan Ren[a], Baoman Li[c,***], Yue Zhu[a,**], Maosheng Xia[a,*]

[a] Department of Orthopaedics, The First Hospital of China Medical University, Shenyang, People's Republic of China
[b] Department of Operating Room, First Affiliated Hospital, China Medical University, Shenyang, People's Republic of China
[c] Practical Teaching Center, School of Forensic Medicine, China Medical University, Shenyang, People's Republic of China

ARTICLE INFO

*Keywords:*
Integrin
ERK
Extracellular matrix
Matrix metalloproteinases
Src

ABSTRACT

Spinal cord injury (SCI) is a serious central nervous system (CNS) trauma that results in permanent and severe disability. The extracellular matrix (ECM) can affect the activation of extracellular signal-regulated kinase 1/2 ($ERK_{1/2}$) by interacting with the ERK integrin subunits. In this study, we built a model of SCI with glial fibrillary acidic protein-green fluorescent protein (GFAP-GFP) and thymus cell antigen 1-yellow fluorescent protein-H (Thy1-YFPH) in mice that express specific transgenes in their astrocytes or neurons. Then, we collected spinal cord neurons or astrocytes by fluorescence-activated cell sorting (FACS). In this way, we investigated the SCI-induced phosphorylation of $ERK_{1/2}$ and epidermal growth factor receptor (EGFR) in neurons and astrocytes, and we discovered that the SCI-induced EGFR signaling pathways differed between neurons and astrocytes. In the present study, we found that the Src-dependent phosphorylation of EGFR induced by SCI occurred only in neurons, not in astrocytes. This phenomenon may be due to the involvement of Thy-1, which promoted the binding between Src and EGFR in neurons after SCI. In addition, the expression of the integrin subunits after SCI differed between neurons and astrocytes. Our present study shows that the EGFR signaling pathway triggered by SCI in neurons differed from the EGFR signaling pathway triggered in astrocytes, a finding that may help to pave the way for clinical trials of therapies that inhibit EGFR signaling pathways after SCI.

## 1. Introduction

Spinal cord injury (SCI) is a serious central nervous system (CNS) trauma that results in permanent and severe disability (Profyris et al., 2004). Crushing injury to the spinal cord is a commonly seen in the clinic and can occur subsequent to traumatic vertebral fracture, intervertebral disk herniation, hematoma, or neoplasia (Sheng et al., 2004). The extracellular matrix (ECM) environment of the CNS is responsible for regulating crucial functions, such as neuronal and glial cell motility, proliferation, and differentiation, by interacting with integrins (Novak and Kaye, 2000; Kearns et al., 2003; Flanagan et al., 2006; Andressen et al., 2005; Kopp et al., 2010). SCI initiates reactive tissue remodeling, including glial scarring, which results from ECM deposition that includes collagen types I, III, and IV; laminin; and fibronectin (Kaneko et al., 2006; Niclou et al., 2006; Schwab et al., 2005a,b). Schachtrup et al. found that the fibrinogen deposited in the spinal cord after

*Abbreviations:* SCI, spinal cord injury; CNS, central nervous system; ECM, extracellular matrix; $ERK_{1/2}$, extracellular signal-regulated kinases 1/2; FACS, fluorescence-activated cell sorting; EGFR, epidermal growth factor receptor; MMPs, matrix metalloproteinases; BSA, bovine serum albumin; PAGE, polyacrylamide gel electrophoresis; ANOVA, analysis of variance; HB-EGF, heparin-binding EGF; FAK, focal adhesion kinase; MAPK, mitogen-activated protein kinase; CSPGs, chondroitin sulfate proteoglycans; Thy-1, thymus cell antigen 1; DNQX, 6,7-dinitroquinoxaline-2,3(1H,4H)-dione; APV, DL-2-amino-5-phosphonopentanoic acid; PP1, 4-amino-5- (4-methylphenyl)-7-(t-butyl)pyrazolo[3,4-d]pyrimidine; U0126, 1,4-diamino-2,3-dicyano-1,4-bis[2-aminophenylthio]butadiene; FN-439, 4-aminobenzoyl-Gly-Pro-D-Leu-D-Ala-NH-OH; PD168393, 4-[(3-bromophenyl)amino]-6-acrylamidoquinazoline

* Corresponding author. Department of Orthopaedics, The First Hospital of China Medical University, No. 155 Nanjing Bei Street, Heping District, Shenyang, 110001, People's Republic of China.
** Corresponding author.
*** Corresponding author.
*E-mail address:* maoshengxia@yahoo.com (M. Xia).
*URLs:* http://bmli@cmu.edu.cn (B. Li), http://zhuyuedr@163.com (Y. Zhu).
[1] These authors are equal to this paper.

https://doi.org/10.1016/j.neuint.2019.104500
Received 16 January 2019; Received in revised form 25 June 2019; Accepted 7 July 2019
Available online 08 July 2019
0197-0186/ 

traumatic injury blocked neurite outgrowth in neurons (Schachtrup et al., 2007). Fibrinogen, an acute-phase reactant, is secreted by hepatocytes in the liver, is present in the blood and can be leaked into the CNS after traumatic injury accompanied by vascular damage or in conjunction with a compromised blood–brain barrier (BBB) (Schachtrup et al., 2007).

Integrins constitute a class of cell adhesion molecules that regulate interactions between a cell and its surrounding matrix (Hynes, 1992). In many cell types, integrins participate in signaling events (Hynes, 2002; Delon and Brown, 2007; Robles and Gomez, 2006), thus controlling gene expression (Hynes, 1992; Ekstrom et al., 2003), the cell cycle (Watt, 2002), and apoptosis (Matter and Ruoslahti, 2001). The presence of α1, α2, α3, α4, α5, α6, α7, β1, and β3 integrin subunits has been documented in neurons (Perez-Martinez and Jaworski, 2005; Dana et al., 2004; Leclere et al., 2007; Gardiner et al., 2005, 2007). Different combinations of α and β subunits give rise to multiple ECM receptors, whose expression is considerably cell type specific (Hynes, 1992). Some of the functions of these subunits have also been proven, and the integrin subunits are critical for interactions with collagens (integrin α1β1 subunit), fibronectin (integrin α5β1 subunit), laminin-10/11 (integrin α3β1 subunit) and laminin-1 (integrin α6β1 subunit) (Mruthyunjaya et al., 2010; Gilchrist et al., 2007). The release of the ECM after stimulation by SCI affects glial scar formation (Okuda et al., 2017) and neurite growth (Duchossoy et al., 2001). Thymus cell antigen 1 (Thy-1), which is a cellular marker for identifying neurons, can bind laminin and fibronectin (Liësi et al., 1990).

Recently, various studies have clearly shown that SCI can induce the phosphorylation or expression of extracellular signal-regulated kinase 1/2 ($ERK_{1/2}$) in neurons or glial cells (Lu et al., 2010; Gao and Ji, 2009; Esposito et al., 2009; Xia et al., 2010). Moreover, some components of the ECM (such as fibronectin and laminin-1) can regulate the activation of the ERK signaling pathways by interacting with integrins (Cui et al., 2006; Lee et al., 2006; Jin et al., 2011; Mendes et al., 2010; Mruthyunjaya et al., 2010; Woods et al., 2001). We previously reported that fibronectin stimulates the activation of $ERK_{1/2}$ and triggers the proliferation of spinal cord astrocytes via integrin α5β1 *in vitro* (Xia and Zhu, 2014). Our previous research and other studies have demonstrated that the ERK signaling pathway can control the specific expression of individual integrin subunits in a variety of cell lines (Xia and Zhu, 2011a,b; Woods et al., 2001; Villa-Garcia et al., 1994; Kang et al., 1999). However, whether the stimulation from the SCI could further regulate the expression of integrin subunits remains unknown. The *in vivo* effects of spinal cord injuries on separated neurons and astrocytes also remain unclear, particularly with respect to cell signaling pathways. Analyzing the respective effects of fibronectin induced by SCI on neurons and astrocytes is beneficial for discussing the therapeutic potential for spinal cord repair.

In this study, after building models of SCI in FVB/NTg(GFAP-GFP) 14Mes/J or B6.Cg-Tg(Thy1-YFPH)2Jrs/J mice, we separated the astrocytes or the neurons by fluorescence-activated cell sorting (FACS) and tested the different signaling pathways induced by the SCI in the neurons and astrocytes. First, we investigated whether the SCI-induced activation of $ERK_{1/2}$ and epidermal growth factor receptor (EGFR) depended on different signaling pathways in the neurons and astrocytes. Then, we showed that the increased expression of integrin subunits differs between neurons and astrocytes. In addition, the phosphorylation of $ERK_{1/2}$ affected the SCI-induced upregulation of integrin subunits.

## 2. Materials and methods

### 2.1. Materials

The chemicals used for preparing media and most other chemicals were purchased from Sigma (St. Louis, MO, USA). PP1 (4-amino-5-(4-methylphenyl)-7-(t-butyl)pyrazolo[3,4-d]pyrimidine), U0126 (1,4-diamino-2,3-dicyano- 1,4-bis[2- aminophenylthio]butadiene), FN-439 (4-aminobenzoyl-Gly-Pro-D-Leu-D-Ala-NH- OH), and PD168393 (4-[(3-bromophenyl)amino]-6-acrylamidoquinazoline) were from Calbiochem (Darmstadt, Germany). For western blotting, the primary antibodies used against integrin α1, α2, α3, α5, α6, β1, and β3; β-actin; and phosphorylated $ERK_{1/2}$ and $ERK_{1/2}$ and the secondary goat anti-rabbit or goat anti-mouse IgG HRP-conjugated antibodies were all purchased from Santa Cruz Biotechnology (Santa Cruz, CA, USA). For immunoprecipitation, the primary antibodies against integrin α1, α2, α3, α5, α6, β1, and β1, as well as the protein G agarose bead slurry, were all purchased from Upstate Biotechnology (Lake Placid, NY, USA). The primary antibodies against EGFR and Src were purchased from Cell Signaling Technology (Danvers, MA, USA), and Thy-1 was purchased from Abcam (Cambridge, MA, USA).

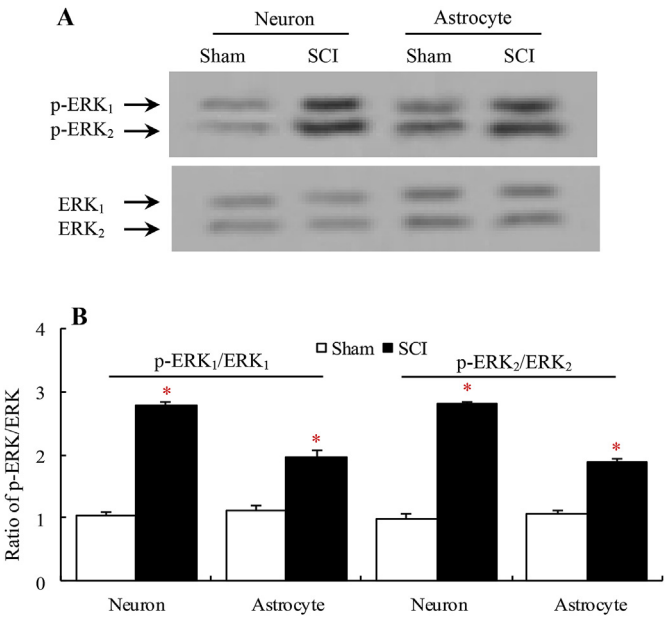


**Fig. 1.** SCI induced ERK phosphorylation in the separated neurons and astrocytes. The Thy1-YFPH or GFAP-GFP mice were pretreated with or without the SCI operation for 3 days, and neurons and astrocytes were separated by FACS. **(A)** Immunoblot from a representative experiment. Similar results were obtained from six independent experiments (cells from 3 mice were mixed as one sample, and six samples were collected independently for each group). The average ERK phosphorylation was quantitated as the ratio between p-$ERK_1$ and $ERK_1$ as well as between p-$ERK_2$ and $ERK_2$ and plotted as a function of SCI **(B)**. The S.E.M. values are indicated by vertical bars, n = 6. *Indicates a statistically significant ($P < 0.05$) difference compared with the sham group for $ERK_1$ and $ERK_2$.

### 2.2. Animals

As described previously (Xia et al., 2017, 2018), B6.Cg-Tg(Thy1-YFP)HJrs/J and FVB/N-Tg(GFAP-GFP)14Mes/J mice were all purchased from the Jackson Laboratory (Bar Harbor, ME, USA). The male mice were selected at an age of approximately 3 months (~25 g) and were kept in standard housing conditions (22 ± 1 °C with a light/dark cycle of 12 h/12 h) with food and water available *ad libitum*. All operations were performed in accordance with the US National Institutes of Health Guide for the Care and Use of Laboratory Animals (NIH Publication No. 8023) and its 1978 revision, and all experimental protocols were approved by the Institutional Animal Care and Use Committee of China Medical University, No. [2019]059.

### 2.3. Spinal cord injury

As described previously (Kuhn and Wrathall, 1998; Erschbamer

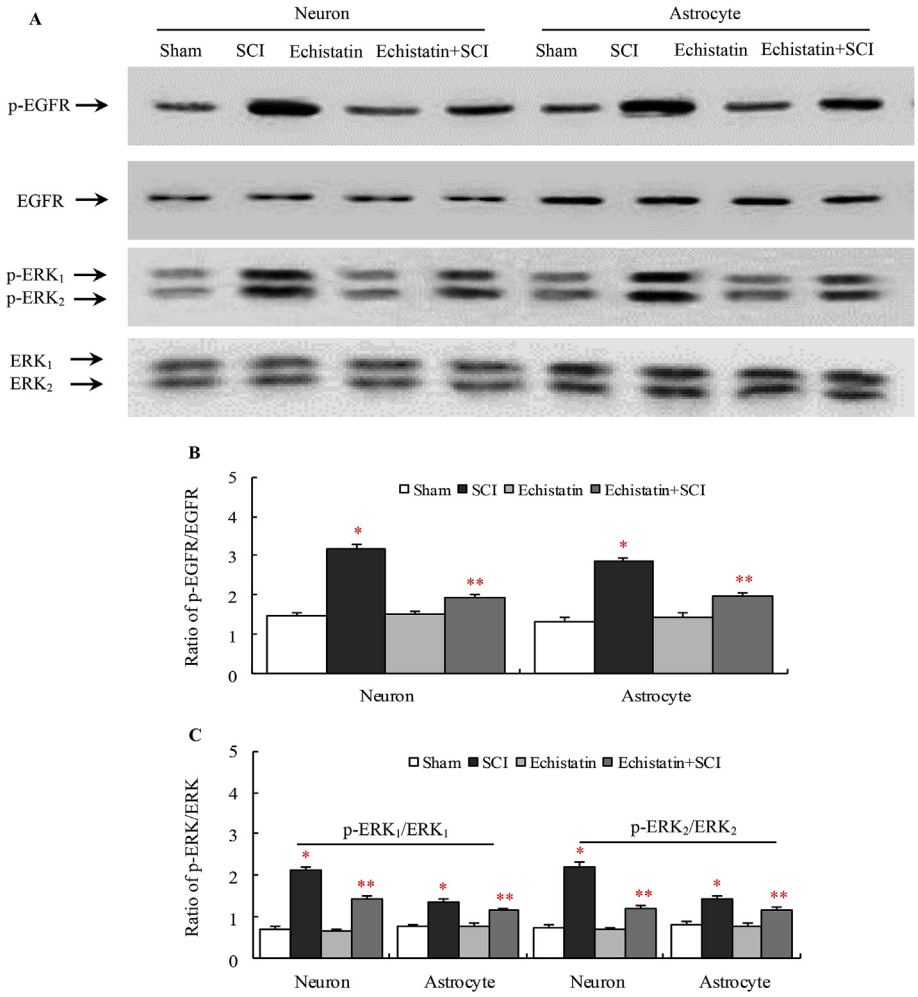


**Fig. 2.** The integrin subunits were required for the phosphorylation of EGFR and ERK in the isolated neurons and astrocytes. Intrathecal injection of echistatin (an integrin αvβ1 inhibitor) at a dose of 10 μg/mouse was performed for the echistatin group and the echistatin with injury group. The Thy1-YFPH or GFAP-GFP mice were pretreated with or without the SCI operation and after 3 days, neurons and astrocytes were separated by FACS. **(A)** Immunoblot from a representative experiment. Similar results were obtained from six independent experiments (cells from 3 mice were mixed as one sample, and six samples were collected independently for each group). The average phosphorylation of EGFR and ERK was quantitated as the following ratios: p-EGFR to EGFR **(B)**, p-$ERK_1$ to $ERK_1$ and p-$ERK_2$ to $ERK_2$, and each was plotted as a function of SCI **(C)**. The S.E.M. values are indicated by vertical bars, n = 6. *Indicates a statistically significant ($P < 0.05$) difference compared with any other group, and **indicates a statistically significant ($P < 0.05$) difference compared with the sham, echistatin and echistatin with SCI groups for EGFR, $ERK_1$ and $ERK_2$.

et al., 2007; Lytle and Wrathall, 2007), surgery was performed on transgenic mice that were 10–12 weeks of age. The mice were anesthetized by inhalation of halothane, and a laminectomy was performed at thoracic level 8–9 to expose the dura. The spinal column was stabilized on the lateral processes at T7 and T10. A contusion was produced by dropping a 10 g weight (rod diameter of 2 mm) on the exposed dura from a height of 1.25 cm. The muscle was sutured, and the skin was closed with wound clips. Sham animals underwent the same surgical procedures except for the SCI, and the surgical incision was sutured. The animals were subsequently injected subcutaneously with 2 mL of saline in the hip area. The animals were placed under a heat lamp during recovery and kept in standard housing conditions. The mouse bladders were manually voided twice a day until the mice recovered normal bladder function. The food and water were arranged near the mice to food and water available *ad libitum*. After 3 days, the mice were executed and the tissues of spinal cord from T1 to L5 section were collected for the subsequent measurements.

### 2.4. Intrathecal injection

All intrathecal injections with 5 μl of drugs were performed in the L5–L6 intervertebral space via a modified direct lumbar puncture under halothane anesthesia as described previously (Kim et al., 2010). To test the phosphorylation of $ERK_{1/2}$, 0.5 μg/mouse PD168393 (a selective inhibitor of EGFR tyrosine kinase), 20 μg/mouse FN-439 (a broad-spectrum matrix metalloproteinase [MMP] inhibitor) (Brown et al., 2007), 0.001 μg/mouse PP1 (a Src family tyrosine kinase inhibitor) (Lee et al., 2003) or 10 μg/mouse echistatin (an integrin αvβ1 inhibitor) was administered 1 h before the SCI procedures. To determine the expression of the integrin subunits, 2 μg/mouse U0126 (a specific inhibitor of $MEK_{1/2}$) was injected 1 h before the injury-inducing procedures and every day post-injury.

### 2.5. Fluorescence-activated cell sorting (FACS)

After the injury operation (3 days), the spinal cord tissues of the FVB/NTg(GFAP-GFP)14Mes/J or B6.Cg-Tg(Thy1-YFPH)2Jrs/J mice were collected from the T1 section to the L5 section. These purification procedures are based on our previously described dissociation (Li et al., 2012; Lundgaard et al., 2015). Three spinal cords from mice undergoing the same treatment were mixed together to create one sample, which was immediately moved to cold Hanks buffer solution containing 3 μM 6,7-dinitroquinoxaline-2,3(1H,4H)-dione (DNQX) and 100 μM DL-2-amino-5-phosphonopentanoic acid (APV). The spinal cord was digested with 8 U/ml papain in $Ca^{2+}$/$Mg^{2+}$-free PIPES/cysteine buffer, pH 7.4, for 1 h at 37 °C and 5% $CO_2$. After one wash, the tissue was further digested with 40 U/ml DNase I in $Mg^{2+}$-containing MEM with 1% bovine serum albumin (BSA) for 15 min at 37 °C and 5% $CO_2$. The tissue was then carefully titrated in cold MEM with 1% BSA and centrifuged over a 90% Percoll gradient (GE Healthcare, Piscataway, NJ) to collect all cells below and including the lipid layer. This cell solution was then further diluted five times with MEM containing 1% BSA and centrifuged to create the pellet. GFP and YFP were excited by a 488 nm laser, and the emissions were measured by 530 nm discrimination filters. The cells were sorted into cold MEM with 1% BSA. The number of neurons or astrocytes obtained in from one sample was 5–10 × $10^6$.

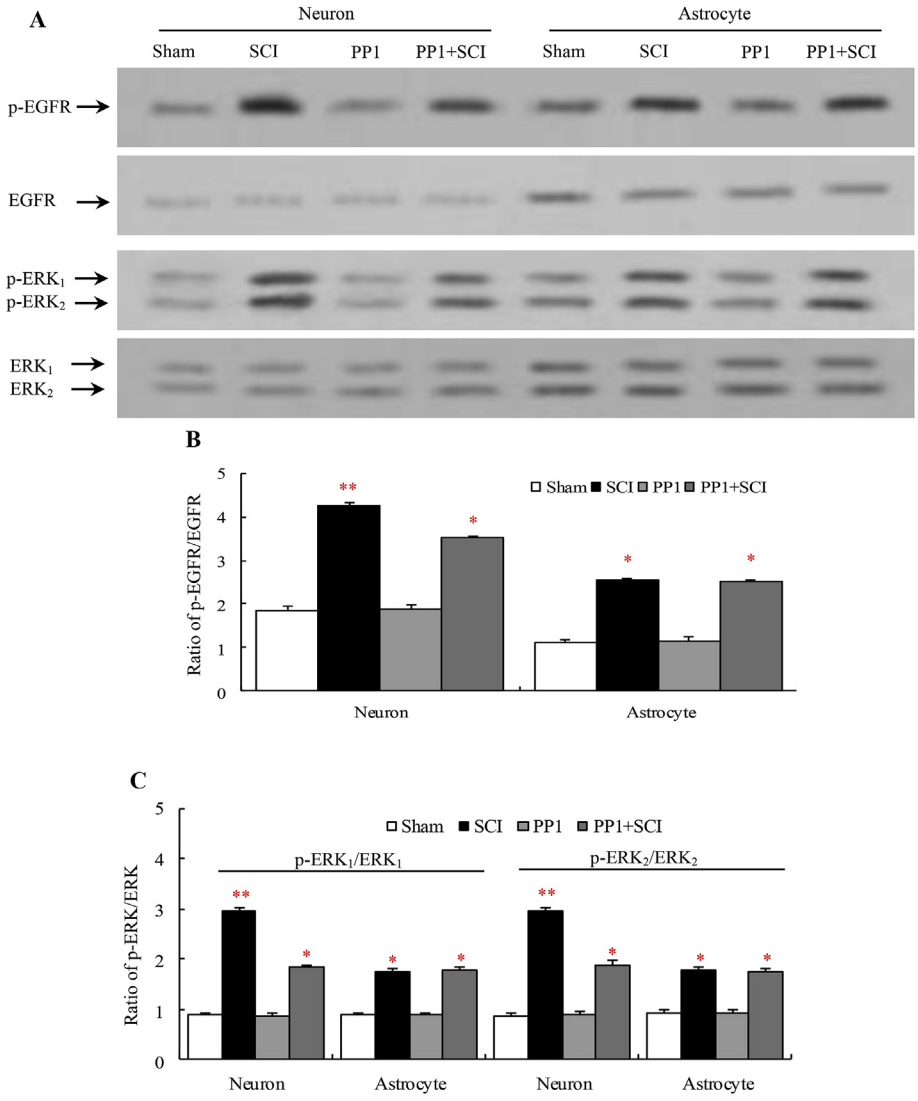


**Fig. 3.** PP1 was not required for the phosphorylation of EGFR or ERK in the separated astrocytes. PP1 (a Src family tyrosine kinase inhibitor) was intrathecally injected into mice of the PP1 group and the PP1 with injury group. The Thy1-YFPH and GFAP-GFP mice were then pretreated with or without SCI operation, and after 3 days, neurons and astrocytes were separated by FACS. **(A)** Immunoblot from a representative experiment. Similar results were obtained from six independent experiments (cells from 3 mice were mixed as one sample, and six samples were collected independently for every group). The average phosphorylation of EGFR and ERK was quantitated as the following ratios: p-EGFR to EGFR **(B)**, p-$ERK_1$ to $ERK_1$ and p-$ERK_2$ to $ERK_2$, and each was plotted as a function of SCI **(C)**. The S.E.M. values are indicated by vertical bars, n = 6. *Indicates a statistically significant ($P < 0.05$) difference compared with the control and the PP1 group for EGFR, $ERK_1$ and $ERK_2$, and **indicates a statistically significant ($P < 0.05$) difference compared with the sham, PP1 and PP1 with SCI groups for EGFR, $ERK_1$ and $ERK_2$.

The mRNA expression of cell-specific markers of neurons (Gabra-1, KCC2 and Snap25), astrocytes (connexin-30, Glt-1 and Fgfr3) or oligodendrocytes (Mag, Mog and Mbp) was evaluated by real-time PCR in the collected neuronal or astrocytic samples. The relative mRNA expression ratios of neuronal markers in the sorted neurons and the positive expression of astrocytic markers in the sorted astrocytes were dramatically higher than the expression ratios of the contaminating cell markers by approximately 30–400 times (please see Supplementary Fig. 1).

### 2.6. Immunoprecipitation and western blotting

After homogenization, the protein content was determined by the Bradford method (Bradford, 1976) using bovine serum albumin as the standard. As described previously (Xia and Zhu, 2011a,b; Xia and Zhu, 2008; Xia and Zhu, 2011a,b), whole cell lysates (500 μg) were incubated with 8 μg of anti-integrin subunits, anti-EGFR or anti-Thy-1 antibody for 12 h at 4 °C. Thereafter, 200 μl of washed protein G agarose bead slurry was added, and the mixture was incubated for another 2 h at 4 °C. The agarose beads were collected by pulsing centrifugation (5 s in the microcentrifuge at 14,000 g), the supernatant was removed, and the beads were boiled for 5 min. Thereafter, the supernatant was collected by pulsing centrifugation, and the entire immunoprecipitate was subjected to 10% SDS-polyacrylamide gel electrophoresis (PAGE). After transfer to nitrocellulose membranes, the samples were blocked with 5% skimmed milk powder in TBS-T (30 mM Tris-HCl, 125 mM NaCl, and 0.1% Tween 20) for 1 h. The nitrocellulose membranes were incubated with the primary antibody specific to the rabbit anti-integrin subunits, EGFR, Thy-1 or Src at a 1:1000 dilution for 2 h at room temperature. After the membranes were washed, the specific binding was detected by a goat anti-rabbit or goat anti-mouse horseradish peroxidase-conjugated secondary antibody at a 1:1000 dilution.

To test the phosphorylation of $ERK_{1/2}$, only western blotting was used. After cell homogenization, the protein content was determined by the Bradford method, and the proteins in the whole cell lysates (50 μg) were separated via SDS-PAGE and then transferred to nitrocellulose membranes. After blocking with 5% skimmed milk, the membrane was incubated with primary anti-p$ERK_{1/2}$ or anti-$ERK_{1/2}$ antibody at a 1:1000 dilution, and then, it was incubated with a goat anti-rabbit or goat anti-mouse horseradish peroxidase-conjugated secondary antibody at a 1:1000 dilution.

Staining was visualized by ECL detection reagents, followed by exposure to film (Fuji Photo Film Co., Ltd., Tokyo, Japan). The results were captured by a FluorChem imaging system (Alpha Innotech Corporation, San Leandro, CA, USA). The band density was measured with Windows AlphaEase™ FC 32-bit software.

### 2.7. Statistical analysis

The differences among multiple groups were analyzed by one-way

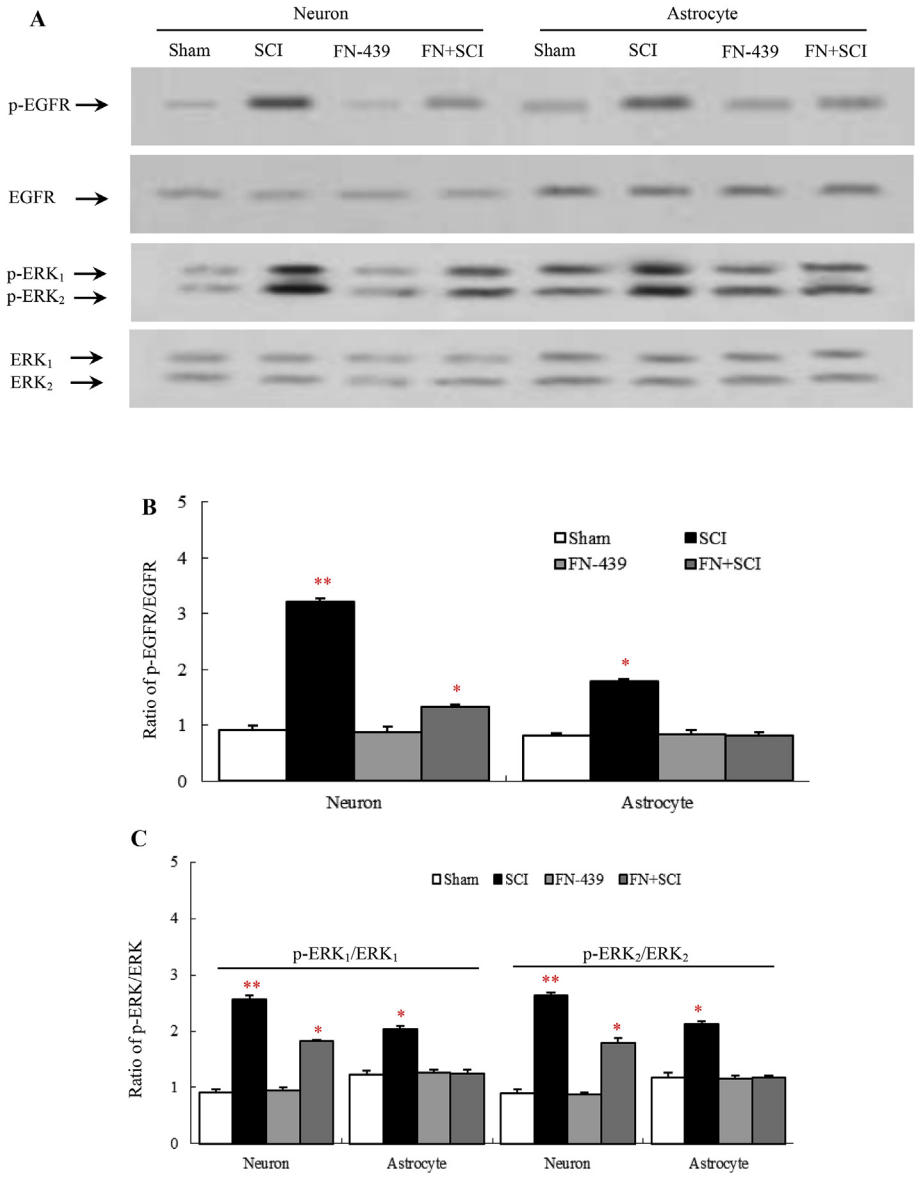


**Fig. 4.** The effect of FN-439 on the phosphorylation of EGFR and ERK in separated neurons and astrocytes. FN-439 (a broad-spectrum MMP inhibitor) was intrathecally injected into the mice of the FN-439 group and the FN-439 with injury group. The Thy1-YFPH or GFAP-GFP mice were then pretreated with or without SCI operation, and after 3 days, the neurons and astrocytes were separated by FACS. **(A)** Immunoblot from a representative experiment. Similar results were obtained from six independent experiments (cells from 3 mice were mixed as one sample, and six samples were collected independently for every group). The average phosphorylation of EGFR and ERK was quantitated as the following ratios: p-EGFR to EGFR **(B)**, p-$ERK_1$ to $ERK_1$ and p-$ERK_2$ to $ERK_2$, and each was plotted as a function of SCI **(C)**. S.E.M. values are indicated by vertical bars, n = 6. *Indicates a statistically significant ($P < 0.05$) difference compared with the control and FN-439 groups for EGFR, $ERK_1$ and $ERK_2$, and **indicates a statistically significant ($P < 0.05$) difference compared with the sham, FN-439 and FN-439 with SCI groups for EGFR, $ERK_1$ and $ERK_2$.

analysis of variance (ANOVA) followed by a Tukey-Kramer post hoc multiple comparison test for unequal replications using GraphPad Prism 5 software (GraphPad Software Inc., La Jolla, CA). All statistical data in the text are expressed as the mean ± S.E.M.; the level of significance was set at $p < 0.05$.

## 3. Results

### 3.1. The SCI induced the phosphorylation of $ERK_{1/2}$ in both the neurons and astrocytes

Fig. 1 shows that the phosphorylation of $ERK_{1/2}$ could have been triggered by the SCI operation as determined in the neurons and astrocytes separated by FACS. Three days after the SCI, the levels of p-$ERK_1$ and p-$ERK_2$ were increased by 172.5 ± 5.1% (n = 6, $p < 0.0001$) and 186.7 ± 5.7% (n = 6, $p < 0.0001$), respectively, in the neurons, and they were also increased by 75.9 ± 4.3% (n = 6, $p < 0.0001$) and 78.1 ± 6.2% (n = 6, $p < 0.0001$), respectively, in the astrocytes. Between 6 h and 3 days after the SCI treatment, we measured the phosphorylation levels of $ERK_{1/2}$ in the sorted neurons and astrocytes. The increased phosphorylation of $ERK_{1/2}$ was triggered starting 6 h after the SCI, and there were no significant differences in the measurements taken at different time points (Supplementary Fig. 2).

### 3.2. The activation of EGFR and ERK was induced by the integrin subunits triggered by the SCI

In the neurons and astrocytes, the phosphorylation of both EGFR and $ERK_{1/2}$ was activated after stimulation by the SCI (Fig. 2). Echistatin, an integrin αvβ1 inhibitor, significantly decreased the levels of p-EGFR and p-$ERK_{1/2}$. In the neurons, the phosphorylation of EGFR in the SCI group was 215.6% ± 11.0% (n = 6, $p < 0.0001$) of that of the sham group, but that level was decreased to 131.1% ± 7.2% (n = 6, p = 0.0027) of that of the sham group after treatment with echistatin (Fig. 2B). In addition, the levels of p-$ERK_1$ and p-$ERK_2$ in the echistatin-treated group were decreased to 201.4% ± 7.5% (n = 6, $p < 0.0001$) and 161.3% ± 8.7% (n = 6, $p < 0.0001$) of the levels in the sham group, respectively (Fig. 2C). Similar results were obtained in the astrocytes, as echistatin suppressed the SCI-induced phosphorylation of EGFR from 217.4% ± 7.7% (n = 6, $p < 0.0001$) to 150.2% ± 7.3% (n = 6, p = 0.0003) of the EGFR phosphorylation levels of the sham group (Fig. 2B). Echistatin also dramatically decreased the levels of p-$ERK_1$ and p-$ERK_2$ to 149.4% ± 5.6% (n = 6, p = 0.0005) and

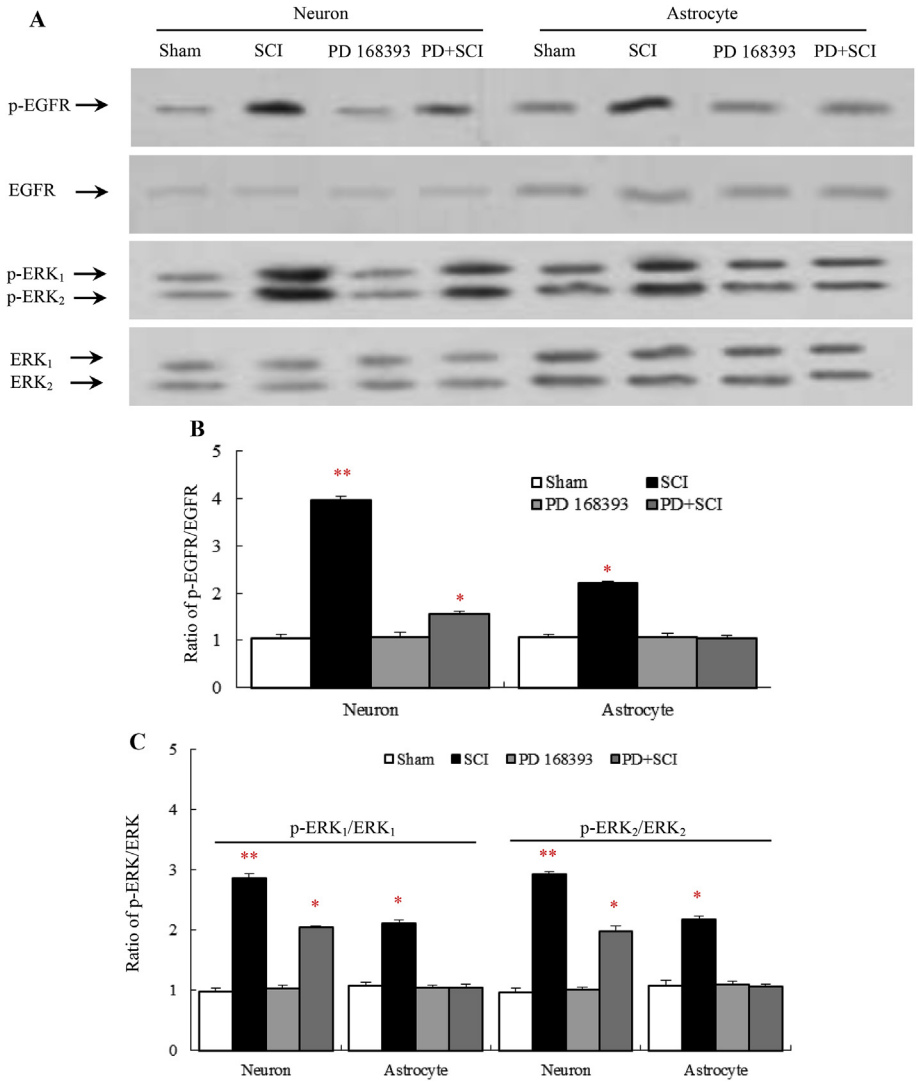


**Fig. 5.** The effect of PD168393 on the phosphorylation of EGFR and ERK in separated neurons and astrocytes. PD168393 (a selective inhibitor of EGFR tyrosine kinase) was intrathecally injected into mice of the PD168393 group and the PD168393 with injury group. The Thy1-YFPH or GFAP-GFP mice were pretreated with or without SCI operation, and after 3 days, neurons and astrocytes were separated by FACS. **(A)** Immunoblot from a representative experiment. Similar results were obtained from six independent experiments (cells from 3 mice were mixed as one sample, and six samples were collected independently for every group). The average phosphorylation of EGFR and ERK was quantitated as the following ratios: p-EGFR to EGFR **(B)**, p-$ERK_1$ to $ERK_1$ and p-$ERK_2$ to $ERK_2$, and each was plotted as a function of SCI **(C)**. The S.E.M. values are indicated by vertical bars, n = 6. *Indicates a statistically significant ($P < 0.05$) difference compared with the control and PD168393 groups for EGFR, $ERK_1$ and $ERK_2$, and **indicates a statistically significant ($P < 0.05$) difference compared with the sham, PD168393 and PD168393 with SCI groups for EGFR, $ERK_1$ and $ERK_2$.

144.4% ± 6.2% (n = 6, p = 0.0069) of those in the sham group, respectively (Fig. 2C).

### 3.3. The signaling pathway associated with SCI-induced $ERK_{1/2}$ phosphorylation differed between neurons and astrocytes

In both neurons and astrocytes, the phosphorylation of EGFR could be stimulated by the SCI (Fig. 3, Fig. 4 and Fig. 5). However, when we injected PP1 (an inhibitor of Src family tyrosine kinases), FN-439 (an inhibitor of MMPs) or PD168393 (an inhibitor of EGFR tyrosine kinase) before the SCI operation, the reduction in EGFR and $ERK_{1/2}$ phosphorylation levels induced by these inhibitors differed between neurons and astrocytes. Fig. 3A shows that PP1 partly decreased the phosphorylation of EGFR by 17.4 ± 1.2% (n = 6, p < 0.0001) in the injury group and reduced the levels of p-$ERK_1$ and p-$ERK_2$ by 36.9 ± 1.1% (n = 6, p < 0.0001) and p-$ERK_2$ by 36.1 ± 3.3% (n = 6, p < 0.0001) in the injury group, respectively, in neurons, but PP1 had no significant effect on the phosphorylation of EGFR or $ERK_{1/2}$ in astrocytes. We also checked the effects of PP1 on the phosphorylation of EGFR and $ERK_{1/2}$ at higher concentrations (0.1 μg/mouse) and found that it did not modulate the increased phosphorylation of EGFR and $ERK_{1/2}$ induced by the SCI in astrocytes (Supplementary Fig. 3). In neurons, FN-439 decreased the phosphorylation of EGFR, $ERK_1$ and $ERK_2$ by 58.3 ± 2.2% (n = 6, p < 0.0001), 29.2 ± 1.2% (n = 6, p < 0.0001) and 31.9 ± 3.1% (n = 6, p < 0.0001), respectively, compared with the phosphorylation levels in the injury group (Fig. 4). However, FN-439 almost completely abolished the activation of EGFR and $ERK_{1/2}$ in astrocytes (Fig. 4). Similar results are presented in Fig. 5 for the phosphorylation of EGFR, which was reduced to 60.6 ± 1.7% (n = 6, p < 0.0001) of EGFR phosphorylation level in the injury group by PD168393, and the phosphorylation levels of p-$ERK_1$ and p-$ERK_2$ were decreased to 28.3 ± 0.7% (n = 6, p < 0.0001) and 32.2 ± 2.9% (n = 6, p < 0.0001) of the phosphorylation level of $ERK_1$ and $ERK_2$ in the injury group, respectively, in neurons; however, PD168393 completely eliminated the phosphorylation of EGFR and $ERK_{1/2}$ in astrocytes.

### 3.4. The formation of the Thy1-Src-EGFR complex was activated in neurons after SCI

In the sorted neurons, we measured the level of Thy-1 linked with Src and EGFR via immunoprecipitation. As shown in Fig. 6, the expression of Thy-1 was not dramatically changed in neurons after SCI. However, the level of Src linked with Thy-1 was clearly increased by 68.1 ± 9.1% (n = 6, p = 0.0008) after SCI compared with the sham procedure, and the level of EGFR linked with Thy-1 or Src was elevated by 658.3 ± 7.2% (n = 6, p < 0.0001) or 266.7 ± 5.4% (n = 6, p < 0.0001), respectively, after SCI.

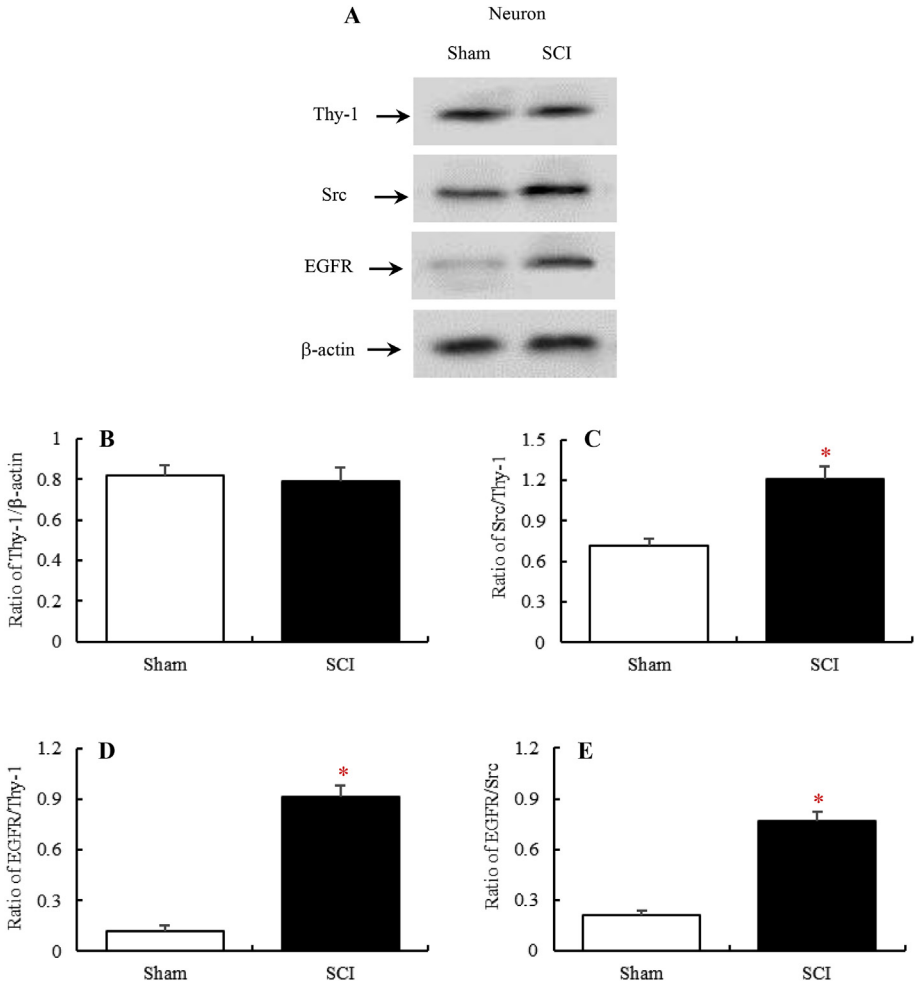


**Fig. 6.** The SCI induced the binding between Src and EGFR via Thy-1 in sorted neurons. The Thy1-YFPH mice were pretreated with or without SCI operation, and after 3 days, neurons were separated by FACS. **(A)** Immunoprecipitation assay was performed with anti-Thy-1, and the western blots for Thy-1, Src, EGFR and β-actin are shown. Immunoblot from a representative experiment. The average level of Thy-1 was quantitated as the ratio of Thy-1 to β-actin (B), the average Src was calculated as the ratio of Src to Thy-1 (C), and the average EGFR was separately compared with Thy-1 (D) and Src (E). The S.E.M. values are indicated by vertical bars, n = 6. *Indicates a statistically significant ($P < 0.05$) difference compared with the sham group.

### *3.5. The increase in the expression levels of integrin subunits after stimulation by SCI differed between neurons and astrocytes*

Fig. 7A shows that integrin subunits α1, α3, α5, α6, β1 and β3 were all increased 3 days after SCI in neurons, but only integrin α3, α6 and β1 were elevated in astrocytes. SCI had no effect on the expression of integrin α1, α5 or β3 in astrocytes. We injected U0126 (an inhibitor of $MEK_{1/2}$) 1 h before SCI, as Fig. 7B shows, which elevated expression of integrin α5 and completely abolished β1 expression. In addition, the expression of integrin α1, α6 and β1 was decreased by 32.9 ± 3.9% (n = 6, p = 0.0169), 70.4 ± 4.1% (n = 6, p < 0.0001) and 63.2 ± 2.8% (n = 6, p < 0.0001) in the injury group, respectively, by U0126, but this inhibitor had no effect on the SCI-induced upregulation of integrin α3 in neurons. In astrocytes, the expression of integrin α3 and β1 was completely eliminated by U0126, but U0126 decreased the expression of integrin α6 by 24.8 ± 4.7% (n = 6, p = 0.0345) in the injury group.

## 4. Discussion

A crushing SCI causes devastating consequences, including lifelong disability and significant economic costs (Profyris et al., 2004). The ECM has been found to be increased in association with secondary damage after a SCI (Koeppen, 2004; Majumdar et al., 2003). Different ECM components, such as laminin-1 and fibronectin, can stimulate the mitogen-activated protein kinase (MAPK)/ERK signaling pathways via their respective integrin subunits (Schachtrup et al., 2007; Mruthyunjaya et al., 2010; Lauro et al., 2006). Because different ECM components have different receptors, there is no inhibitor or antagonist that can block all ECM receptors. We used echistatin (an inhibitor of the integrin αvβ1 receptor) to determine whether fibronectin, a main component of the ECM, is involved in the neuronal stimulation induced by the SCI. The results demonstrate that the integrin αvβ1 receptor was a partial requirement for the phosphorylation of EGFR and $ERK_{1/2}$, as shown in Fig. 2. However, other ECM substrates have specific integrin subunits in their receptors, and the functions of these integrin subunits may differ because the regulatory signaling pathways through which they function in neurons may differ from the pathways through which they function in astrocytes.

In this study, we found that the signaling pathway of the transactivated EGFR and $ERK_{1/2}$ as mediated by Src differed between the neurons and astrocytes after SCI. This specific signaling pathway in the neurons may be attributed to the effects induced by Thy-1, which makes Thy-1 useful for identifying neurons. The activated ECM proteins induced by the SCI, such as laminin and fibronectin, may stimulate Thy-1 in neurons (Liësi et al., 1990). Thy-1 can activate Src by associating with the C-terminal Src kinase (Csk)-binding protein (CBP) in neurons (Maldonado et al., 2017). Src activates the phosphorylation of EGFR in the company of Src/EGFR (Du et al., 2010). In this study, treatment with SCI promoted the binding between Src and EGFR through Thy-1 in neurons. After SCI, the members of the Src kinase family, which includes c-Src, Lck, Fgr, Yes, Fyn, Hck and Lyn, PP1 effectively blocked Src kinase activity *in vitro* and *in vivo*, and it did not discriminate between different members of this family (Bartscht et al., 2017). After SCI, the exact members of the Src family involved in the effects of the ECM still awaiting further determination. Furthermore, whether these other signaling pathways or molecules that are induced by SCI have different or completely converse functions requires further investigation, even in

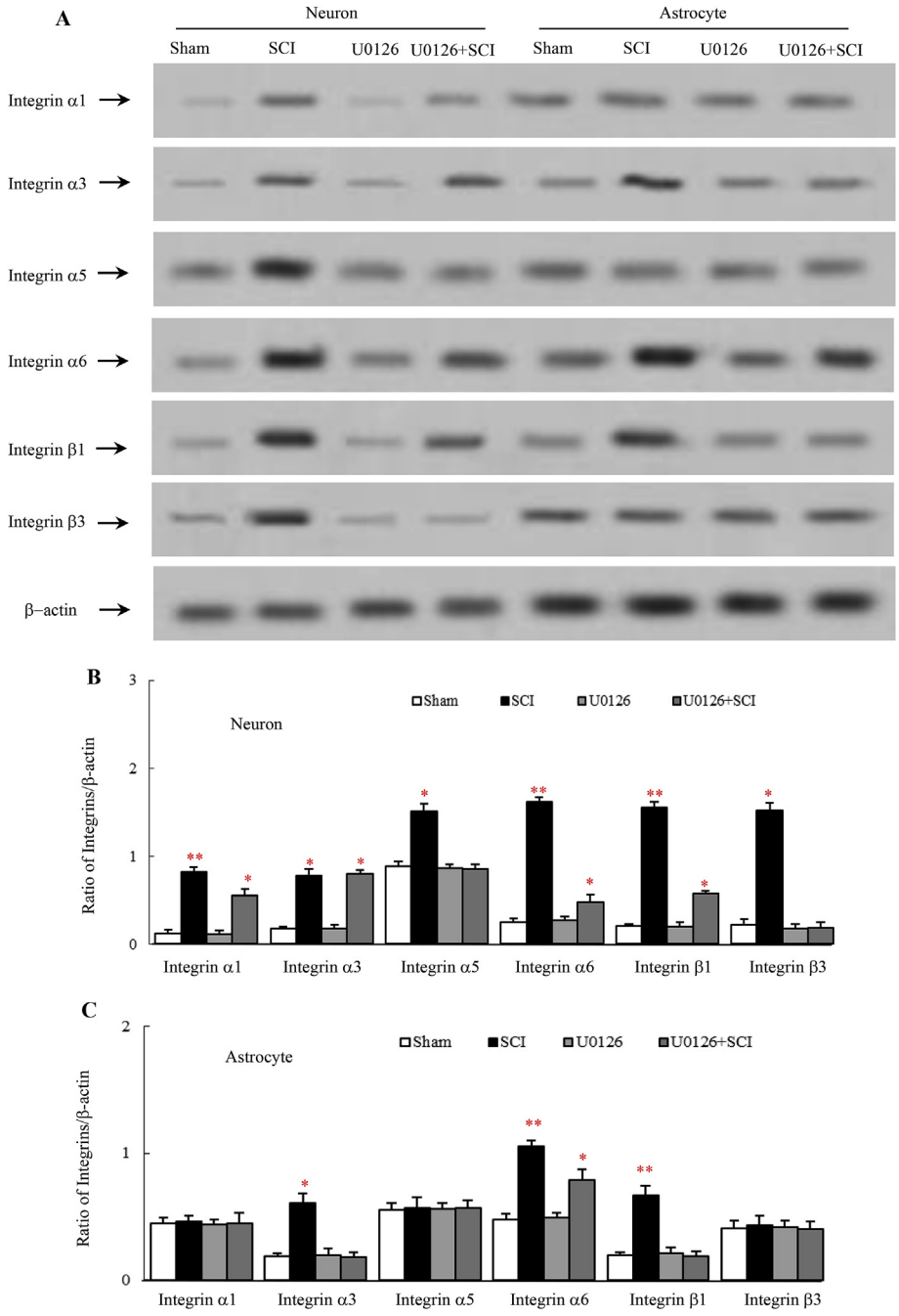


**Fig. 7.** The protein expression of the integrin subunits in separated neurons and astrocytes. U0126 (a specific inhibitor of $MEK_{1/2}$) was intrathecally injected into mice of the U0126 group and the U0126 with injury group. The Thy1-YFPH or GFAP-GFP mice were pretreated with or without SCI operation, and after 3 days, neurons and astrocytes were separated by FACS. **(A)** Immunoblot from a representative experiment. Similar results were obtained from six independent experiments (cells from 3 mice were mixed as one sample, and six samples were collected independently for each group). The average protein levels of the integrin subunits were quantitated as the ratios of each integrin subunit to β-actin in neurons **(B)** and in astrocytes **(C)**. The S.E.M. values are indicated by vertical bars, n = 6. *Indicates a statistically significant ($P < 0.05$) difference compared with the sham and U0126 groups for integrin subunits, **indicates a statistically significant ($P < 0.05$) difference compared with the sham, U0126 and U0126 with SCI groups for the integrin subunits.

different neuronal cells, because the activation of ERK has also been reported in microglia after SCI, with specific involvement in inflammatory response (Fu et al., 2018).

In this study, individual inhibitors, e.g., PP1, FN-439 and PD168393, did not have the same effects on neurons as they did on astrocytes. We injected the inhibitors intrathecally, as described previously (Kim et al., 2010; Lee et al., 2007). For each inhibitor, the injected dose and protocol were identical for the Thy1-YFP and GFAP-GFP mice. After 1 h, the distribution of the inhibitors in the spinal cord was balanced. Therefore, the different functions as observed in neurons and astrocytes were not attributed to experimental error.

The MAPK pathway in mammals consists of $ERK_{1/2}$, c-Jun N-terminal kinase (JNK), p38, and $ERK_5$ (Wang et al., 2019). Inflammation stimulates the activation of the MAPK signaling system, and the phosphorylation levels of ERK and p38 is different in neurons than in astrocytes. The phosphorylation of ERK is induced in both neurons and astrocytes, but the phosphorylation of p38 is present only in neurons (Worsley et al., 2014). However, as we previously reported, because fibronectin promotes the proliferation of the spinal cord astrocytes by enhancing the activation of $ERK_{1/2}$ in the primarily culture astrocytes of spinal cord (Xia and Zhu, 2014), we mainly investigated the effects of the ECM on the regulation of $ERK_{1/2}$ in neurons and astrocytes after SCI. Our study also discovered differences in the transactivation of EGFR and downstream ERK signaling pathways. We speculate that these differences may be attributed to the effect of Thy-1, which could promote the linkage between Src and EGFR to increase the activation of EGFR in neurons.

The present observations also revealed the differential expression of the integrin subunits in neurons and astrocytes. Schachtrup et al. reported that fibrinogen acts as a ligand for integrin β3 and induces the transactivation of EGFR in spinal cord neurons (Schachtrup et al., 2007). In human cancer cells, the activation of ERK induces the

expression of integrin α6 and β3 (Woods et al., 2001). Elevated levels of surface integrins are associated with increased neurite outgrowth (Condic, 2001; Wallquist et al., 2004), and increased integrin expression following neuronal injury is correlated with the successful regeneration of peripheral neurons (Previtali et al., 2001) and with limited regeneration of central neurons after neurotrophin treatment (Plantman et al., 2005). In this study, integrin α5β1, which was inhibited by echistatin, was partly involved in the effects of the ECM on the transactivation of EGFR and $ERK_{1/2}$ both in neurons and astrocytes. In human umbilical vein endothelial cells, fibronectin induces the expression of MMP-9 by stimulating Src-mediated ERK, thereby promoting the degradation of collagen and leading to a change in the ECM structure and to angiogenesis (Jin et al., 2011).

After adhesion to the ECM, the integrin subunits in the plane of the plasma membrane activate various protein tyrosine kinases (such as focal adhesion kinase [FAK], Src and Abl) and serine-threonine kinases (such as MAPK and protein kinase C) (Clark and Brugge, 1995; Schwartz, 1997; Howe et al., 1998). The various signaling pathways of EGFR that are induced by SCI may produce the different effects observed in neurons and astrocytes. In the spinal cord, the activation of EGFR triggers astrocytes to become reactive astrocytes (Liu et al., 2006), and EGFR ligands stimulate the secretion of chondroitin sulfate proteoglycans (CSPGs) (Smith and Strunz, 2005), as well as the formation of cribriform astrocyte arrangements that might contribute to the formation of glial scars (Liu and Neufeld, 2004). In our previous study, fibronectin enhanced the spinal cord astrocyte proliferation that was mediated by the EGFR-ERK signaling pathway via the integrin α5β1 receptor (Xia and Zhu, 2014). Autocrine fibronectin from mesenchymal stem cells triggers neurite growth and promotes nerve fiber regeneration after SCI (Zeng et al., 2016). Moreover, the increased integrin subunits in neurons and/or astrocytes may further promote the functions of the ECM triggered by SCI.

In this study, the transactivation of EGFR-ERK contributed to the growth of neurons and astrocytes, but astrocyte overgrowth facilitated the formation of glial scars after SCI. After blocking the classical transactivation of EGFR induced by SCI *in vivo*, the only remaining pathway existed in neurons: Src-activated EGFR transactivation may enable fibronectin or other elements of the ECM to promote neurite outgrowth; thus, the formation of glial scars could be suppressed to improve the injury recovery of patients. The observed differences in the EGFR signaling pathways induced by SCI between neurons and astrocytes may help pave the way for clinical trials of agonists or inhibitors of the EGFR signaling pathway in the treatment of SCI.

## Conflicts of interest

The authors have no conflicts of interest to disclose.

## Acknowledgments

This study was supported by Grant No. 81200935 to MX from the National Natural Science Foundation of China, Grant No. 20170541030 to MX from the Natural Science Foundation of Liaoning Province, Grant No. 81871852 to BL from the National Natural Science Foundation of China, Grant No. XLYC1807137 to BL from LiaoNing Revitalization Talents Program, and Grant No. 20151098 to BL from the Scientific Research Foundation for Overseas Scholars of the Education Ministry of China.

## Appendix A. Supplementary data

Supplementary data to this article can be found online at https://doi.org/10.1016/j.neuint.2019.104500.

## References

Andressen, C., Adrian, S., Fässler, R., Arnhold, S., Addicks, K., 2005. The contribution of beta1 integrins to neuronal migration and differentiation depends on extracellular matrix molecules. Eur. J. Cell Biol. 84, 973–982.
Bartscht, T., Rosien, B., Rades, D., Kaufmann, R., Biersack, H., Lehnerta, H., Ungefroren, H., 2017. Inhibition of TGF-β signaling in tumor cells by small molecule Src family kinase inhibitors. Anti Cancer Agents Med. Chem. 17, 1351–1356.
Bradford, M.M., 1976. A rapid and sensitive method for the quantitation of microgram quantities of protein utilizing the principle of protein-dye binding. Anal. Biochem. 72, 248–254.
Brown, T.E., Forquer, M.R., Cocking, D.L., Jansen, H.T., Harding, J.W., Sorg, B.A., 2007. Role of matrix metalloproteinases in the acquisition and reconsolidation of cocaine-induced conditioned place preference. Learn. Mem. 14, 214–223.
Clark, E.A., Brugge, J.S., 1995. Integrins and signal transduction pathways: the road taken. Science 268, 233–239.
Condic, M., 2001. Adult neuronal regeneration induced by transgenic integrin expression. J. Neurosci. 21, 4782–4788.
Cui, Y., Chen, Y., Zhi, J.L., Guo, R.X., Feng, J.Q., Chen, P.X., 2006. Activation of p38 mitogen-activated protein kinase in spinal microglia mediates morphine antinociceptive tolerance. Brain Res. 1069, 235–243.
Dana, L.N., William, J.R., Setton, L.A., 2004. Integrin expression in cells of the intervertebral disc. J. Anat. 204, 515–520.
Delon, I., Brown, N.H., 2007. Integrins and the actin cytoskeleton. Curr. Opin. Cell Biol. 19, 43–50.
Du, T., Li, B., Li, H., Li, M., Hertz, L., Peng, L., 2010. Signaling pathways of isoproterenol-induced $ERK_{1/2}$ phosphorylation in primary cultures of astrocytes are concentration-dependent. J. Neurochem. 115, 1007–1023.
Duchossoy, Y., Horvat, J.C., Stettler, O., 2001. MMP-related gelatinase activity is strongly induced in scar tissue of injured adult spinal cord and forms pathways for ingrowing neurites. Mol. Cell. Neurosci. 17, 945–956.
Ekstrom, P.A., Mayer, U., Panjwani, A., Pountney, D., Pizzey, J., Tonge, D.A., 2003. Involvement of alpha7beta1 integrin in the conditioning-lesion effect on sensory axon regeneration. Mol. Cell. Neurosci. 22, 383–395.
Erschbamer, M., Pernold, K., Olson, L., 2007. Inhibiting epidermal growth factor receptor improves structural, locomotor, sensory, and bladder recovery from experimental spinal cord injury. J. Neurosci. 27, 6428–6435.
Esposito, E., Genovese, T., Caminiti, R., Bramanti, P., Meli, R., Cuzzocrea, S., 2009. Melatonin reduces stress-activated/mitogen-activated protein kinases in spinal cord injury. J. Pineal Res. 4679–4686.
Flanagan, L.A., Rebaza, L.M., Derzic, S., Schwartz, P.H., Monuki, E.S., 2006. Regulation of human neural precursor cells by laminin and integrins. J. Neurosci. Res. 83, 845–856.
Fu, X., Shen, Y., Wang, W., Li, X., 2018. MiR-30a-5p ameliorates spinal cord injury-induced inflammatory responses and oxidative stress by targeting Neurod 1 through MAPK/ERK signalling. Clin. Exp. Pharmacol. Physiol. 45, 68–74.
Gao, Y.J., Ji, R.R., 2009. c-Fos and pERK, which is a better marker for neuronal activation and central sensitization after noxious stimulation and tissue injury? Open Pain J. 2, 11–17.
Gardiner, N.J., Fernyhough, P., Tomlinson, D.R., Mayer, U., von der, Mark, H., Streuli, C.H., 2005. Alpha7 integrin mediates neurite outgrowth of distinct populations of adult sensory neurons. Mol. Cell. Neurosci. 28, 229–240.
Gardiner, N.J., Moffatt, S., Fernyhough, P., Humphries, M.J., Streuli, C.H., Tomlinson, D.R., 2007. Preconditioning injury-induced neurite outgrowth of adult rat sensory neurons on fibronectin is mediated by mobilisation of axonal alpha5 integrin. Mol. Cell. Neurosci. 32, 249–260.
Gilchrist, C.L., Chen, J., Richardson, W.J., Loeser, R.F., Setton, L.A., 2007. Functional integrin subunits regulating cell–matrix interactions in the intervertebral disc. J. Orthop. Res. 25, 829–840.
Howe, A., Aplin, A.E., Alahari, S.K., Juliano, R.L., 1998. Integrin signaling and cell growth control. Curr. Opin. Cell Biol. 10, 220–231.
Hynes, R.O., 1992. Integrins: versatility, modulation, and signaling in cell adhesion. Cell 69, 11–25.
Hynes, R.O., 2002. Integrins: bidirectional, allosteric signaling machines. Cell 110, 673–687.
Jin, Y.J., Park, I., Hong, I.K., Byun, H.J., Choi, J., Kim, Y.M., Lee, H., 2011. Fibronectin and vitronectin induce AP-1-mediated matrix metalloproteinase-9 expression through integrin α(5)β(1)/α(v)β(3)-dependent Akt, ERK and JNK signaling pathways in human umbilical vein endothelial cells. Cell. Signal. 23, 125–134.
Kaneko, S., Iwanami, A., Nakamura, M., Kishino, A., Kikuchi, K., Shibata, S., Okano, H.J., Ikegami, T., Moriya, A., Konishi, O., Nakayama, C., Kumagai, K., Kimura, T., Sato, Y., Goshima, Y., Taniguchi, M., Ito, M., He, Z., Toyama, Y., Okano, H., 2006. A selective Sema3A inhibitor enhances regenerative responses and functional recovery of the injured spinal cord. Nat. Med. 12, 1380–1389.
Kang, C.D., Do, I.R., Kim, K.W., Ahn, B.K., Kim, S.H., Chung, B.S., Jhun, B.H., Yoo, M.A., 1999. Role of Ras/ERK-dependent pathway in the erythroid differentiation of K562 cells. Exp. Mol. Med. 31, 76–82.
Kearns, S.M., Laywell, E.D., Kukekov, V.K., Steindler, D.A., 2003. Extracellular matrix effects on neurosphere cell motility. Exp. Neurol. 182, 240–244.
Kim, D., You, B., Jo, E.K., Han, S.K., Simon, M.I., Lee, S.J., 2010. NADPH oxidase 2-derived reactive oxygen species in spinal cord microglia contribute to peripheral nerve injury-induced neuropathic pain. Proc. Natl. Acad. Sci. U. S. A. 107, 14851–14856.
Koeppen, A.H., 2004. Wallerian degeneration: history and clinical significance. J. Neurol. Sci. 220, 115–117.
Kopp, M.A., Brommer, B., Gatzemeier, N., Schwab, J.M., Prüss, H., 2010. Spinal cord

injury induces differential expression of the profibrotic semaphorin 7A in the developing and mature glial scar. Glia 58, 1748–1756.
Kuhn, P.L., Wrathall, J.R., 1998. A mouse model of graded contusive spinal cord injury. J. Neurotrauma 15, 125–140.
Lauro, C., Catalano, M., Trettel, F., Mainiero, F., Ciotti, M.T., Eusebi, F., Limatola, C., 2006. The chemokine CX3CL1 reduces migration and increases adhesion of neurons with mechanisms dependent on the beta1 integrin subunit. J. Immunol. 177, 7599–7606.
Leclere, P.G., Norman, E., Groutsi, F., Coffin, R., Mayer, U., Pizzey, J., Tonge, D., 2007. Impaired axonal regeneration by isolectin B4-binding dorsal root ganglion neurons in vitro. J. Neurosci. 27, 1190–1199.
Lee, I., Kim, H.K., Kim, J.H., Chung, K., Chung, J.M., 2007. The role of reactive oxygen species in capsaicin-induced mechanical hyperalgesia and in the activities of dorsal horn neurons. Pain 133, 9–17.
Lee, K.K., de, Repentigny, Y., Saulnier, R., Rippstein, P., Macklin, W.B., Kothary, R., 2006. Dominant-negative beta1 integrin mice have region-specific myelin defects accompanied by alterations in MAPK activity. Glia 53, 836–844.
Lee, M.C., Smith, F.L., Stevens, D.L., Welch, S.P., 2003. The role of several kinases in mice tolerant to delta 9-tetrahydrocannabinol. J. Pharmacol. Exp. Ther. 305, 593–599.
Li, B., Dong, L., Wang, B., Cai, L., Jiang, N., Peng, L., 2012. Cell type-specific gene expression and editing responses to chronic fluoxetine treatment in the in vivo mouse brain and their relevance for stress-induced anhedonia. Neurochem. Res. 37, 2480–2495.
Liësi, P., Salonen, E.M., Dahl, D., Vaheri, A., Richards, S.J., 1990. Thy-1 is a neuronal and glial surface antigen which interacts with matrix proteins and plasminogen activator. Exp. Brain Res. 79, 642–650.
Liu, B., Chen, H., Johns, T.G., Neufeld, A.H., 2006. Epidermal growth factor receptor activation: an upstream signal for transition of quiescent astrocytes into reactive astrocytes after neural injury. J. Neurosci. 26, 7532–7540.
Liu, B., Neufeld, A.H., 2004. Activation of epidermal growth factor receptor causes astrocytes to form cribriform structures. Glia 46, 153–168.
Lu, K., Liang, C.L., Liliang, P.C., Yang, C.H., Cho, C.L., Weng, H.C., Tsai, Y.D., Wang, K.W., Chen, H.J., 2010. Inhibition of extracellular signal-regulated kinases 1/2 provides neuroprotection in spinal cord ischemia/reperfusion injury in rats: relationship with the nuclear factor-kappaB-regulated anti-apoptotic mechanisms. J. Neurochem. 114, 237–246.
Lundgaard, I., Li, B., Xie, L., Kang, H., Sanggaard, S., Haswell, J.D., Sun, W., Goldman, S., Blekot, S., Nielsen, M., Takano, T., Deane, R., Nedergaard, M., 2015. Direct neuronal glucose uptake Heralds activity-dependent increases in cerebral metabolism. Nat. Commun. 6, 6807.
Lytle, J.M., Wrathall, J.R., 2007. Glial cell loss, proliferation and replacement in the contused murine spinal cord. Eur. J. Neurosci. 25, 1711–1724.
Majumdar, M.K., Keane-Moore, M., Buyaner, D., Hardy, W.B., Moorman, M.A., McIntosh, K.R., Mosca, J.D., 2003. Characterization and functionality of cell surface molecules on human mesenchymal stem cells. J. Biomed. Sci. 10, 228–241.
Maldonado, H., Calderon, C., Burgos-Bravo, F., Kobler, O., Zuschratter, W., Ramirez, O., Härtel, S., Schneider, P., Quest, A.F., Herrera-Molina, R., Leyton, L., 2017. Astrocyte-to-neuron communication through integrin-engaged Thy-1/CBP/Csk/Src complex triggers neurite retraction via the RhoA/ROCK pathway. Biochim. Biophys. Acta Mol. Cell Res. 1864, 243–254.
Matter, M.L., Ruoslahti, E., 2001. A signaling pathway from the alpha5beta1 and alpha(v) beta3 integrins that elevates bcl-2 transcription. J. Biol. Chem. 276, 27757–27763.
Mendes, K.N., Wang, G.K., Fuller, G.N., Zhang, W., 2010. JNK mediates insulin-like growth factor binding protein 2/integrin alpha5-dependent glioma cell migration. Int. J. Oncol. 37, 143–153.
Mruthyunjaya, S., Manchanda, R., Godbole, R., Pujari, R., Shiras, A., Shastry, P., 2010. Laminin-1 induces neurite outgrowth in human mesenchymal stem cells in serum/differentiation factors-free conditions through activation of FAK-MEK/ERK signaling pathways. Biochem. Biophys. Res. Commun. 391, 43–48.
Niclou, S., Ehlert, E.M., Verhaagen, J., 2006. Chemorepellent axon guidance molecules in spinal cord injury. J. Neurotrauma 23, 409–421.
Novak, U., Kaye, A.H., 2000. Extracellular matrix and the brain: components and function. J. Clin. Neurosci. 7, 280–290.
Okuda, A., Horii-Hayashi, N., Sasagawa, T., Shimizu, T., Shigematsu, H., Iwata, E., Morimoto, Y., Masuda, K., Koizumi, M., Akahane, M., Nishi, M., Tanaka, Y., 2017. Bone marrow stromal cell sheets may promote axonal regeneration and functional recovery with suppression of glial scar formation after spinal cord transection injury in rats. J. Neurosurg. Spine 26, 388–395.
Perez-Martinez, L., Jaworski, D.M., 2005. Tissue inhibitor of metalloproteinase-2 promotes neuronal differentiation by acting as an anti-mitogenic signal. J. Neurosci. 25, 4917–4929.
Plantman, S., Novikova, L., Novikov, L., Hammarberg, H., Wallquist, W., Kellerth, J.O., Cullheim, S., 2005. Integrin messenger RNAs in the red nucleus after axotomy and neurotrophic administration. Neuroreport 16, 709–713.
Previtali, S.C., Feltri, M.L., Archelos, J.J., Quattrini, A., Wrabetz, L., Hartung, H., 2001. Role of integrins in the peripheral nervous system. Prog. Neurobiol. 64, 35–49.
Profyris, C., Cheema, S.S., Zang, D., Azari, M.F., Boyle, K., Petratos, S., 2004. Degenerative and regenerative mechanisms governing spinal cord injury. Neurobiol. Dis. 15, 415–436.
Robles, E., Gomez, T.M., 2006. Focal adhesion kinase signaling at sites of integrin-mediated adhesion controls axon pathfinding. Nat. Neurosci. 9, 1274–1283.
Schachtrup, C., Lu, P., Jones, L.L., Lee, J.K., Lu, J., Sachs, B.D., Zheng, B., Akassoglou, K., 2007. Fibrinogen inhibits neurite outgrowth via beta 3 integrin-mediated phosphorylation of the EGF receptor. Proc. Natl. Acad. Sci. U.S.A. 104, 11814–11819.
Schwab, J., Conrad, S., Monnier, P.P., Julien, S., Mueller, B.K., Schluesener, H.J., 2005a. Spinal cord injury-induced lesional expression of the repulsive guidance molecule (RGM). Eur. J. Neurosci. 21, 1569–1576.
Schwab, J.M., Monnier, P.P., Schluesener, H.J., Conrad, S., Beschorner, R., Chen, L., Meyermann, R., Mueller, B.K., 2005b. Central nervous system injury-induced repulsive guidance molecule expression in the adult human brain. Arch. Neurol. 62, 1561–1568.
Schwartz, M.A., 1997. Integrins, oncogenes, and anchorage in-dependence. J. Cell Biol. 139, 575–578.
Sheng, H., Wang, H., Homi, H.M., Spasojevic, I., Batinic-Haberle, I., Pearlstein, R.D., Warner, D.S., 2004. A no-laminectomy spinal cord compression injury model in mice. J. Neurotrauma 21, 595–603.
Smith, G.M., Strunz, C., 2005. Growth factor and cytokine regulation of chondroitin sulfate proteoglycans by astrocytes. Glia 52, 209–218.
Villa-Garcia, M.L., Li, G., Riely, P.F., Bray, P.F., 1994. Isolation and characterization of a TATA-less promoter for the human beta 3 integrin gene. Blood 83, 668–676.
Wallquist, W., Zelano, J., Plantman, S., Kaufman, S.J., Cullheim, S., Hammarberg, H., 2004. Dorsal root ganglion neurons up-regulate the expression of laminin-associated integrins after peripheral but not central axotomy. J. Comp. Neurol. 480, 162–169.
Wang, X.L., Yuan, K., Zhang, W., Li, S.X., Gao, G.F., Lu, L., 2019 Mar 11. Regulation of circadian genes by the MAPK pathway: implications for rapid antidepressant action. Neurosci. Bull. https://doi.org/10.1007/s12264-019-00358-9. [Epub ahead of print].
Watt, F.M., 2002. Role of integrins in regulating epidermal adhesion, growth and differentiation. EMBO J. 21, 3919–3926.
Woods, D., Cherwinski, H., Venetsanakos, E., Bhat, A., Gysin, S., Humbert, M., Bray, P.F., Saylor, V.L., McMahon, M., 2001. Induction of beta3-integrin gene expression by sustained activation of the Ras-regulated Raf-MEK-extracellular signal-regulated kinase signaling pathway. Mol. Cell. Biol. 21, 3192–3205.
Worsley, M.A., Allen, C.E., Billinton, A., King, A.E., Boissonade, F.M., 2014. Chronic tooth pulp inflammation induces persistent expression of phosphorylated ERK (pERK) and phosphorylated p38 (pp38) in trigeminal subnucleus caudalis. Neuroscience 269, 318–330.
Xia, M., Li, X., Yang, L., Ren, J., Sun, G., Qi, S., Verkhratsky, A., Li, B., 2018. The ameliorative effect of fluoxetine on neuroinflammation induced by sleep deprivation. J. Neurochem. 146, 63–75.
Xia, M., Yang, L., Sun, G., Qi, S., Li, B., 2017. Mechanism of depression as a risk factor in the development of Alzheimer's disease: the function of AQP4 and the glymphatic system. Psychopharmacology (Berl) 234, 365–379.
Xia, M., Zhu, Y., 2008. Expression of integrin subunits in the herniated intervertebral disc. Connect. Tissue Res. 49, 464–469.
Xia, M., Zhu, Y., 2011a. Fibronectin fragment activation of ERK increasing integrin $\alpha_5$ and $\beta_1$ subunit expression to degenerate nucleus pulposus cells. J. Orthop. Res. 29, 556–561.
Xia, M., Zhu, Y., 2011b. Signaling pathways of ATP-induced PGE2 release in spinal cord astrocytes are EGFR transactivation-dependent. Glia 59, 664–674.
Xia, M., Zhu, Y., 2014. Fibronectin enhances spinal cord astrocyte proliferation by elevating P2Y1 receptor expression. J. Neurosci. Res. 92, 1078–1090.
Xia, Y., Liu, H., Shen, A., Liu, Y., Sun, L., Tao, T., Ke, Q., Cheng, C., 2010. A critical role of SRC-suppressed C kinase substrate in rat astrocytes after chronic constriction injury. NeuroMolecular Med. 12, 205–216.
Zeng, X., Ma, Y.H., Chen, Y.F., Qiu, X.C., Wu, J.L., Ling, E.A., Zeng, Y.S., 2016. Autocrine fibronectin from differentiating mesenchymal stem cells induces the neurite elongation in vitro and promotes nerve fiber regeneration in transected spinal cord injury. J. Biomed. Mater. Res. A. 104, 1902–1911.